

# The determination of velocity fluctuations in shear flows by means of PTV

by

G. Gullo <sup>(1)</sup>, G. Querzoli <sup>(2)</sup>, M. Moroni <sup>(3)</sup>, G.P. Romano <sup>(1)</sup>

<sup>(1)</sup> Dept. Mechanics and Aeronautics, University "La Sapienza", Roma, Italy  
[romano@dma.uniroma1.it](mailto:romano@dma.uniroma1.it)

<sup>(2)</sup> Dip. Ingegneria del Territorio, University of Cagliari, Italy  
[querzoli@unica.it](mailto:querzoli@unica.it)

<sup>(3)</sup> Dept. Hydraulics, University "La Sapienza", Roma, Italy  
[monica.moroni@uniroma1.it](mailto:monica.moroni@uniroma1.it)

## ABSTRACT

The present study considers the effects of some parameters in image acquisition and analysis procedures in connection with the use of the Particle Tracking Velocimetry (PTV) technique. The interest is focused towards flow fields with large velocity gradients as shear flows; in the paper, velocity measurements by PTV are performed in a turbulent channel flow upstream and downstream of a backward facing step at low Reynolds numbers. This is a flow field largely investigated in the past with available numerical and experimental to make comparison with. Among the possible parameters to be chosen in particle image acquisition and analysis, the following are considered

- the concentration of seeding particles in the imaged region;
- the spatial resolution of the image acquisition system;
- the parameters used in the image analysis algorithm.

An example of the average streamlines downstream of the step is given in figure 1; on the same figure the mean axial velocity profiles upstream of the step obtained using increasing seeding particle concentrations ( $N_3 > N_2 > N_1$ ) are given and compared to numerical results. The main conclusion of the paper is that the selection of parameters for PTV measurements is crucial during the phase of image acquisition, while this is not so much true in the phase of image analysis. In particular, the seeding tracer concentration and the camera spatial resolution are the most relevant parameters to be taken into account.

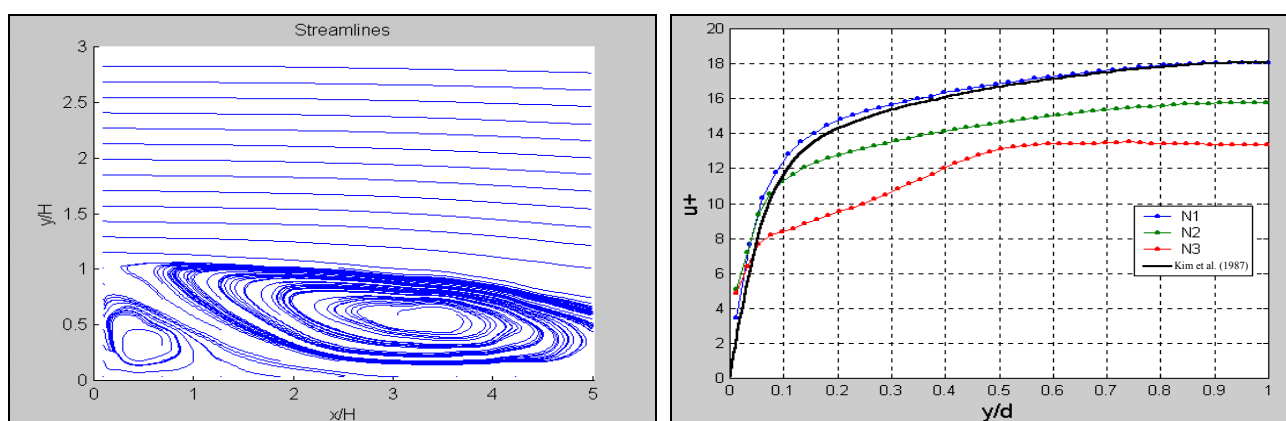


Fig.1. An example of averaged streamlines downstream the step at  $Re = 5400$  (on the left) and the mean axial velocity profiles upstream the step at  $Re = 4100$  (on the right) at different particle concentrations;  $H$  is the step height and  $d$  is the channel half height. The black line reproduces the DNS data by Kim et al. (1987).

## 1. MOTIVATION AND OBJECTIVES

Nowadays, the investigation of complex velocity fields by means of Particle Imaging techniques as PIV (Particle Image Velocimetry) and PTV (Particle Tracking Velocimetry) is able to provide very accurate results especially when several images acquired in the same flow conditions are averaged. On the other hand, on instantaneous plots several “erroneous” data are observed; they result from incorrect evaluations performed by cross-correlation (in PIV) or tracking (in PTV) algorithms. Sometimes, these are corrected using post-processing validation criteria which replace erroneous data through spatial averages on neighbours or on the whole image (Westerweel, 1997, 1999). Of course, this procedures could be highly questionable and could lead to strong errors when looking at higher order statistics (as *rms* velocity fluctuations and Reynolds stresses) or at small scales quantities derived from instantaneous image itself (as vorticity or derivatives in general). Motivations for such erroneous evaluations of the imaging algorithms are

1. the concentration of seeding particles in the imaged region (or sub-region);
2. the size and density of the seeding particles;
3. the quality of the acquired images;
4. the time interval between exposures and/or the flow velocity in the image plane;
5. the spatial resolution of the image acquisition system;
6. the parameters used in the image analysis algorithm.

Among them, the points 1 and 2 concern the set-up and occur before the measurements (tracers), points 3 to 5 with the image acquisition phase and point 6 with the image analysis procedure (Malik *et al.* 1993, Veber *et al.* 1997, Ohmi and Li 2000, Ishikawa *et al.* 2000). In this paper, the attention will be focused on points 1, 5 and 6 which are not suggested with common empirical arguments or relations (unless points 2, 3 and 4).

As far as it concerns point 1, the concentration of seeding particles is crucial for the application of a particular image analysis technique; the quantity which has been used as indicator of the seeding concentration is the number of particles within the region of analysis ( $A_0$ ),

$$N_0 = N_p (A_0 / A) , \quad (1)$$

where  $N_p$  is the number of particles within the whole image ( $A$ ) (Adrian, 1991). For random particle distribution, the probability for particle presence within  $A_0$  is Poisson type *i.e.* dependent only on  $N_0$ ; for  $N_0 \ll 1$  the PTV limit is obtained, while  $N_0 \gg 1$  identifies working conditions for PIV. However, there is still a large range between these two limits in which the performances of the techniques have to be tested.

Regarding point 5, it is well known that especially the data obtained from PIV, due to the finite correlation-window size, are smoothed in space in comparison to those derived from other velocity measurement techniques; typically the spatial resolution is not higher than  $10^3 \text{ m}^{-1}$ , while for Laser Doppler Anemometry (LDA) and Hot Wire Anemometry it is respectively 10 and 100 times larger (Adrian 1991, Westerweel 1999). The problem of the effective size of the „measurement volume“ is particularly severe in flow regions where large velocity gradients occur and these are just the most complex and often interesting ones. Advanced PIV algorithms allow to reduce this problem using correlation window deformation, re-shaping and/or windowing (Keane *et al.* 1995, Nogueira *et al.* 1999, Scarano & Riethmuller 1999, 2000, Di Florio *et al.* 2002). The problem is also present in PTV measurements especially when the original data are re-interpolated on a regular grid to derive the Eulerian statistics. The spatial resolution of Particle Imaging techniques can be increased by:

- reducing the size of the imaged region;
- enhancing the resolution of the image acquisition device;
- using advanced image analysis procedures.

For a given imaging device and image analysis algorithm, the spatial resolution is simply related to the size of the imaged region.

For point 6, depending on the specific algorithm, there are several parameters which affect the quality of the results. In PIV, examples are the window size, the maximum window offsets, the peak detection method, while in PTV they are the maximum and minimum acceptable particle size, the limits for the first and successive particle displacements and the threshold level to be applied to the images.

The present study considers the previous three points (1, 5 and 6) with special interest for PTV measurements in flow fields with large velocity gradients as in shear flows. Velocity measurements are taken in a turbulent channel flow upstream and downstream of a backward facing step at low Reynolds numbers. This is a flow field largely investigated in the past and available numerical and experimental data are used for comparisons upstream and downstream of the step (Armaly *et al.* 1983, Kim *et al.* 1987, Kasagi *et al.* 1992, Le *et al.* 1997, Tumbiolo *et al.* 1999). The aim of the paper is to establish what are the main parameters to be controlled in image acquisition and analysis using PTV.

## 2. EXPERIMENTAL SET-UP

Velocity measurements on a  $(x, y)$  vertical plane ( $x$  is taken streamwise,  $y$  along the vertical and  $z$  spanwise) are performed in a turbulent channel flow close to a backward facing step; upstream of the step (at  $x = -4H$ , where  $H = 1$  cm is the step height and  $x = 0$  identifies the position of the step), the data are acquired and compared with available DNS data (Kim *et al.* 1987), whereas downstream of the step with LDA data (Tumbiolo *et al.* 1999). To ensure a fully developed turbulent flow, the step is located at  $80d$  from the inlet section ( $d = 1$  cm, is the channel half height). To test the effect of the spatial resolution, the size of the measurement region downstream of the step is changed; image acquisition is performed over regions with size between 1.5 cm and 6 cm, i.e. 1.5 and 6 step heights. The data are acquired at Reynolds numbers equal to about 5000 (as the data in the literature); the reference lengths are the channel half height ( $d$ ) for measurements upstream of the step and the step height ( $H$ ) for those downstream of the step, while in the same conditions the reference velocities are the friction velocity ( $u^*$ , equal to 3.0 cm/s) and the maximum velocity ( $U_{\max}$ , equal to 41 cm/s) respectively. A sketch of the experimental set-up is given in figure 2, where the whole hydraulic circuit is shown (the measurement region is located at point  $D$ ); the working fluid is water.

The test section is illuminated by a light sheet (thickness equal to about 1 mm) obtained from an infrared continuous laser (power = 16 W, wavelength = 800 nm) using spherical and cylindrical lenses. The light scattered by pollen particles (diameter = 40  $\mu\text{m}$ , density = 1.06 g/cm<sup>3</sup>) is acquired by a high-speed video-camera (frame rate = 250 Hz, resolution = 480  $\times$  420) and transferred on a PC for further analysis. About 10000 images have been acquired in each condition. As a consequence of the camera resolution and of the imaged area, the spatial resolutions ( $SR$ ) of the acquired data are the following; about 80 cm<sup>-1</sup> upstream of the step and about 25 cm<sup>-1</sup> and 15 cm<sup>-1</sup> for the two imaged area downstream of the step (the spatial resolution is computed as the inverse of the imaged region size divided by the number of cells where velocity vectors are measured). Therefore, comparisons between the results obtained with different spatial resolutions are made possible downstream of the step. The concentration of seeding particles (as defined in equation (1)) is changed between  $N_0 \approx 0.5$  and  $N_0 \approx 20$  (assuming  $A_0 = \pi d_{\max}^2$ , where  $d_{\max}$  is the maximum radius for the first displacement). The concentration is changed upstream and downstream of the step.

The PTV algorithm performs a frame by frame tracking procedure to derive particle displacements and trajectories. Particles are individuated after applying a threshold level on the images, by locating the connected sets of pixels exceeding the threshold; their positions are computed as the average of the pixel locations weighted by their grey levels. A minimum area is requested for the particles to be validated. Tracking is performed on the base of a maximum displacement and of a maximum acceleration; nevertheless, the first constrain is required only for the first step of a trajectory. It must be noticed that no *a priori* information on the expected displacement direction must be provided; thus the algorithm is suitable for trajectory recognition even in turbulent fields without a dominant mean velocity, as in the case of large scale vortices (Cenedese and Querzoli 1997, Cenedese and Querzoli 2000). In summary, the parameters which are used in the PTV algorithm are the following:

- maximum expected first displacement ( $d_{\max}$ );
- tolerance on successive displacements ( $tol$ );
- threshold on intensity levels ( $thres$ );
- minimum accepted area for validated particle barycentre ( $A_{\min}$ ).

As a peculiar feature of PTV, the resulting velocity data are obtained at random positions in space; thus, to compute Eulerian statistics they are projected on a regular grid. So far, in addition to the previous parameters, in post-processing there is also the number of interpolation cells used in the projection.

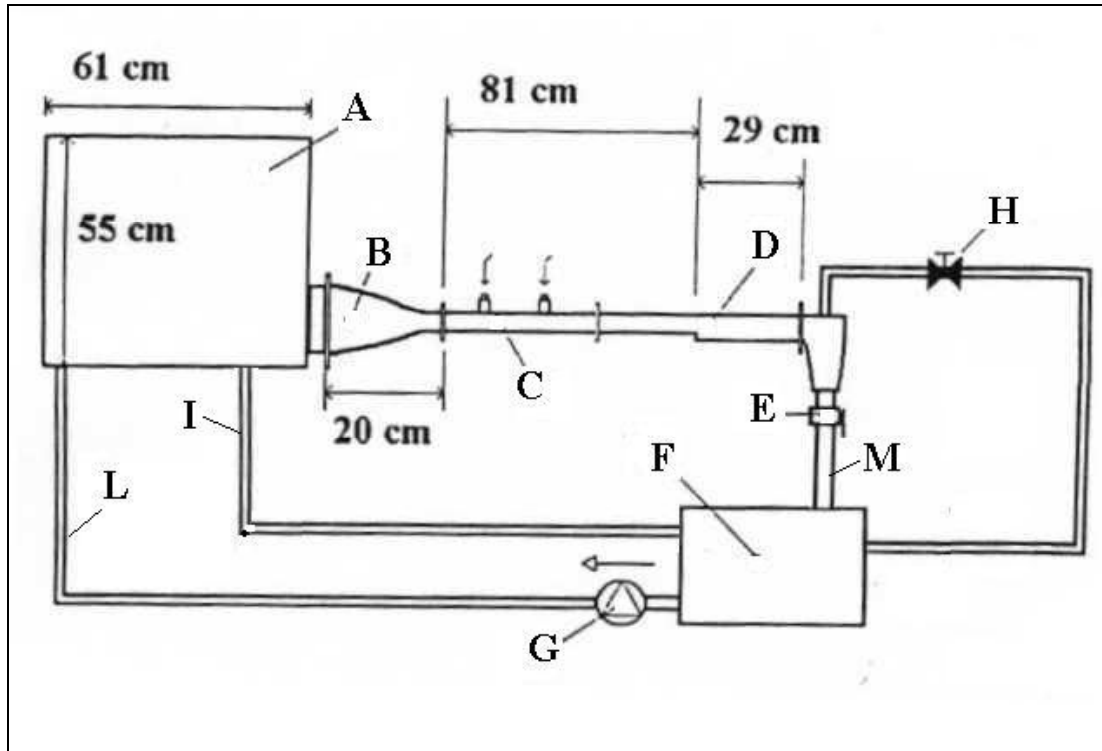


Fig. 2. The schematic diagram of the experimental set-up for velocity measurements upstream and downstream of a backward facing step. The measurement section is located in D, B is the convergent, C is the upstream channel (with holes for dye and tracers) whereas A and F are reservoirs. The velocity in the measurement section is controlled by the valves in E and H, G is the re-circulating pump and I, L, M are connecting pipes.

An example of image processing is given on figures 3 and 4 for the flow upstream of the step (figure 3) and downstream of the step (figure 4). Upstream of the step, a fully developed channel flow should be measured; in the first part of figure 3 the detected trajectories (over about 100 frames) are almost rectilinear due to the careful selection of the previous parameters to avoid “crossings” between trajectories. On average, particle displacements are followed consecutively over about 10 frames. In the second part of the same figure, the measured velocity vectors on a single frame are shown; the number of data is larger than 200 with a small number of noticeable “erroneous” vectors. On the third part of figure 3, the previous vectors at random positions are projected onto a regular (20×30) grid and averaging over 500 frames is performed (as given before, the total number of frames used for the results presented in the next section is 10000).

Similarly, in the first part of figure 4 the detected trajectories (even in this case over 100 frames) are shown for the region just downstream of the step (from  $x/H = 0$  to  $x/H = 5$ ). In this region, the flow exhibits a large re-circulation close to the step where tracer particles are in a smaller number than in the external region (Etheridge and Kemp 1978, Armaly *et al.* 1983, Huang and Fiedler 1997). On average, particle displacements are followed on a about 5 frames; this number is smaller than the one obtained upstream of the step due the strongly three-dimensional nature of the flow field (even if two-dimensional on average). In the second part of figure 4, the velocity vectors derived on a single frame are given; in this case, the number of detected vectors is higher than before (to allow a large number of vectors to be measured in the lowest part of the field the particle concentration is also higher). More than 500 vectors are measured; however, the number of noticeable “erroneous” vectors is higher than those obtained upstream of the step. On the third part of the same figure, the projection on a (20×30) regular grid is given; averaging is performed over 500 frames; the overall expected features of the flow field seem to be captured. A more quantitative analysis on the measurement is presented in the next sections; in particular, in section 3, the analysis of the flow field upstream of the step is presented, whereas in section 4 the analysis is performed downstream of the step.

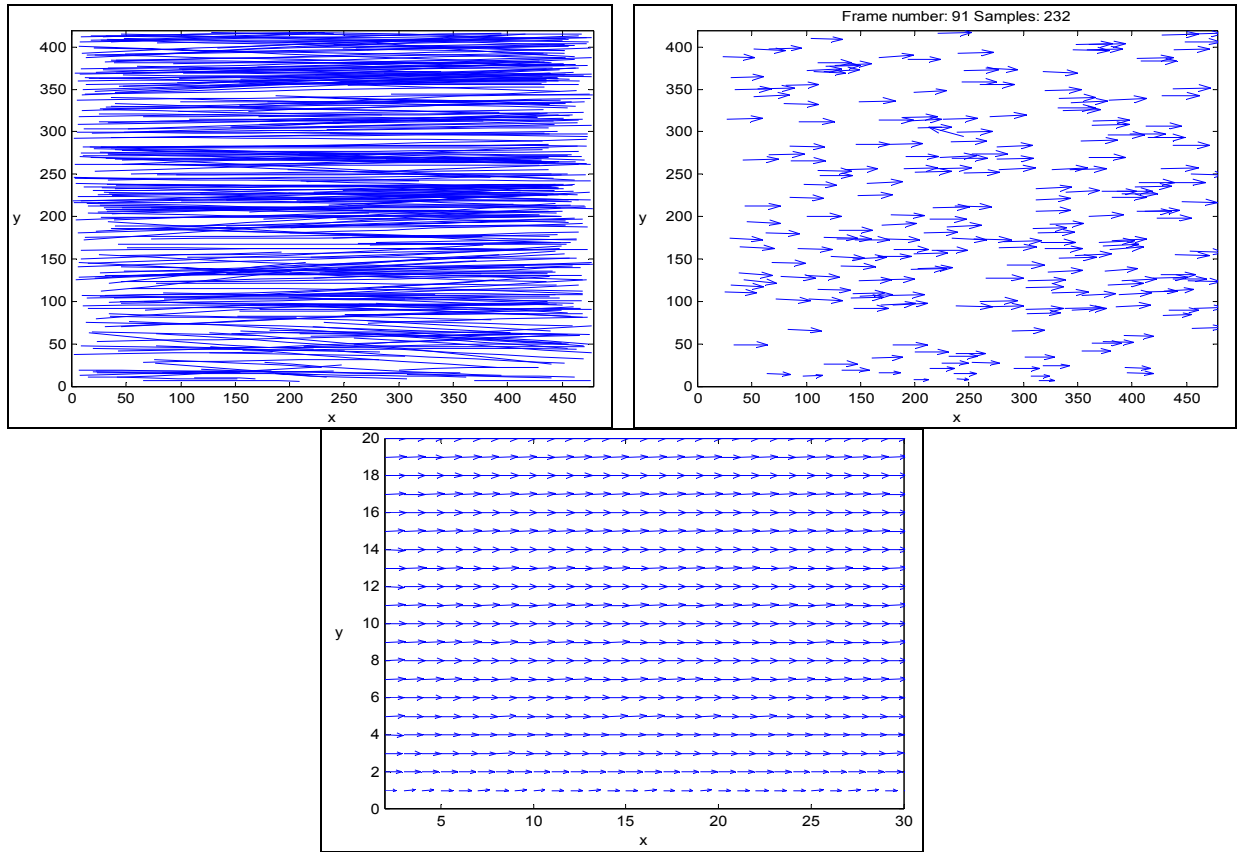


Fig.3. Example of image processing upstream of the step.

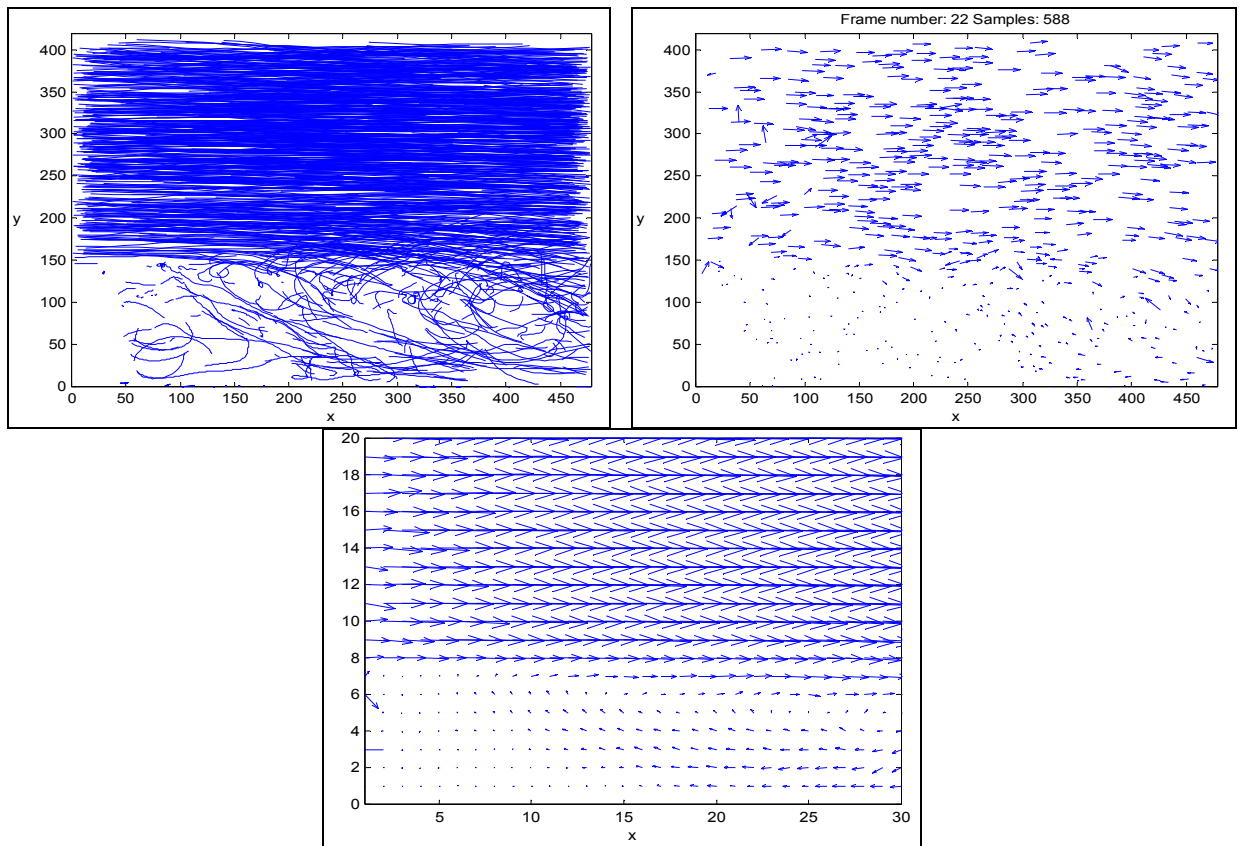


Fig.4. Example of image processing downstream of the step.

### 3. RESULTS UPSTREAM OF THE STEP; EFFECT OF THE PARTICLE CONCENTRATION AND OF THE IMAGE ANALYSIS PARAMETERS

The results obtained upstream of the step are compared with those obtained by Kim *et al.* (1987) using Direct Numerical Simulation (DNS) at almost the same Reynolds number (5400); in figure 5, vertical profiles of the mean axial velocity, *rms* axial and vertical fluctuations and of the main Reynolds stress tensor component are given for different particle concentrations (see Eq. (1));  $N_1 = 4.6$ ,  $N_2 = 14.9$  and  $N_3 = 51.2$ . So far, we move from a particle concentration rather good for PTV to a value which is much more suited for PIV. In the profile of the mean axial velocity, as the concentration increases the measured velocity decreases in comparison to the DNS data by Kim *et al.* (1987); this is due to the fact that the image analysis software validates several almost vertical erroneous trajectories which have a velocity component along the streamwise axis much smaller than the straight ones. On the other hand, contributions from these erroneous measurements increase the *rms* values along the axis and vertically as observed in the *rms* profile given in figure 5. For such profiles, the data obtained with the intermediate particle concentration ( $N_2$ ) are still close to the numerical data. The situation is similar for the Reynolds stress profile, where a strong departure from the other data is obtained for measurements at the highest particle concentration ( $N_3$ ). It should be remarked that for all the profiles, the results obtained at the lowest particle concentration ( $N_1$ ) are very close to the numerical data.

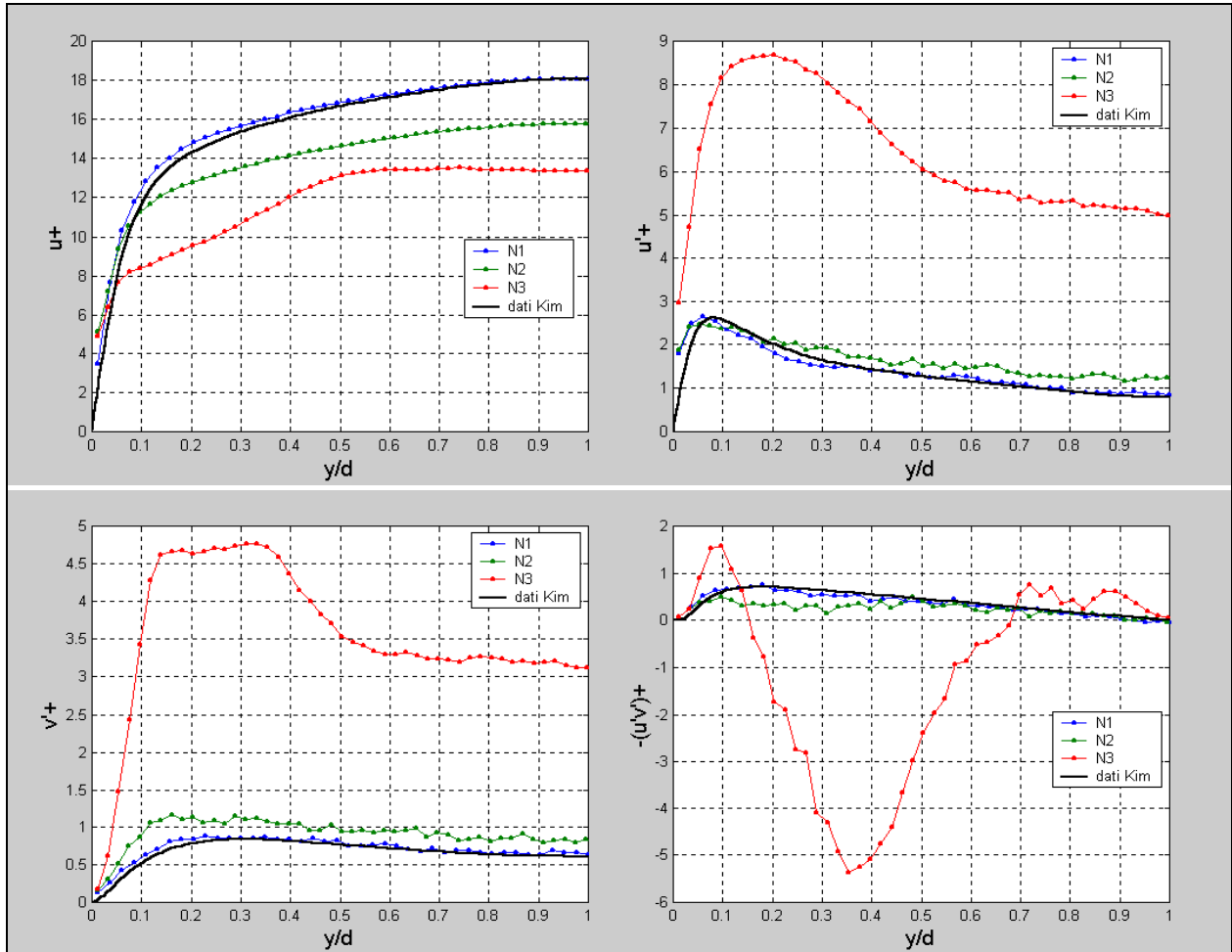


Fig.5. Mean axial velocity, *rms* axial fluctuation profiles (at the top) and *rms* vertical fluctuation and Reynolds stress profiles (at the bottom) obtained at three different particle concentrations (equation (1));  $N_1 = 4.6$ ,  $N_2 = 14.9$  and  $N_3 = 51.2$ . Data acquired at  $Re = 5400$  upstream of the step, with the following parameters;  $SR$  (spatial resolution) =  $80 \text{ cm}^{-1}$ ,  $d_{max}/tol$  (ratio between maximum displacement and tolerance) = 60,  $thres$  (threshold level) = 40,  $A_{min}$  (minimum particle area) =  $2 \text{ pixel}^2$ . The number of cells used is about 80 in each direction.

The second effect considered in this paper concerns with the parameters used in image analysis in the PTV algorithm. In particular, among the others, the effect of the maximum expected displacement ( $d_{\max}$ ) and of the tolerance on successive displacements ( $tol$ ) are considered, while the effects of the threshold intensity level ( $thres$ ) and of the minimum accepted area ( $A_{\min}$ ) are very small (except for the pixel locking effect which is reduced when  $A_{\min} > 6$  pixel<sup>2</sup>). As a matter of fact, the tolerance, non-dimensional by the maximum displacement ( $tol/d_{\max}$ ), is an indicator of the maximum expected velocity fluctuation within the test section; the effect of changes in the value of the non-dimensional tolerance (namely of the inverse,  $d_{\max}/tol$ ) are considered in the following (it should be remarked that variations of  $d_{\max}$  show very small effects except for the case in which large particle displacements are missed in the velocity probability density distributions). In figure 6, the profiles of the same statistical quantities given in figure 5 are shown; the ratio  $d_{\max}/tol$  changes from 60 (which means that the displacement between first and second frame is 60 times larger than the maximum expected variation in successive displacements, *i.e.* the maximum expected turbulence intensity is about 2% (1/60)) to 12 (maximum turbulence intensity equal to 8%). The mean axial velocity profile is almost unaffected by variations of the previous ratio; this means that the number of erroneous trajectories detected with a low  $d_{\max}/tol$  is not large. On the other hand, *rms* profiles deviate from the numerical data in the outer part of the wall layer ( $y/d \geq 0.2$ ) if the maximum expected turbulence fluctuations are larger than 4% ( $d_{\max}/tol < 30$ ); this is due to the fact that the detected erroneous trajectories are present especially towards the centre of the channel.

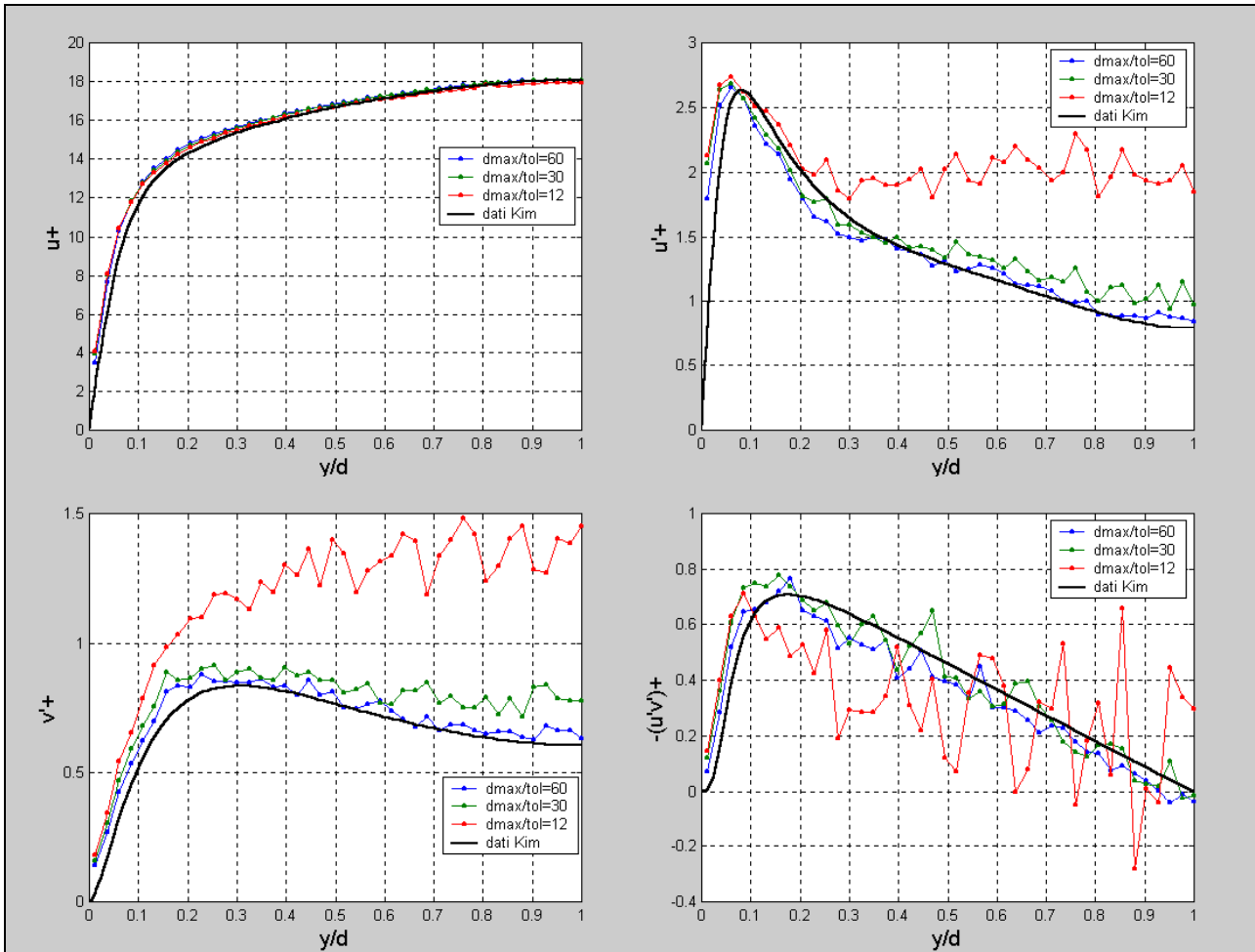


Fig.6. Mean axial velocity, rms axial fluctuation profiles (at the top) and rms vertical fluctuation and Reynolds stress profiles (at the bottom) obtained at three different ratios between maximum displacement and tolerance;  $d_{\max}/tol = 12, 30, 60$ . Data acquired at  $Re = 5400$  upstream of the step, with the following parameters; SR (spatial resolution) =  $80\text{ cm}^{-1}$ ,  $N_0$  (particle concentration) = 4.6,  $thres$  (threshold level) = 40,  $A_{\min}$  (minimum particle area) = 2 pixel<sup>2</sup>. The number of cells used is about 80 in each direction.

The measured Reynolds stress profile does not show any systematic deviation from the numerical data for increasing maximum expected turbulence intensity; rather an increasing random oscillation around the expected behaviour is observed which points out the increasing “incoherent” nature of the detected velocity components moving far from the wall.

#### 4. RESULTS DOWNSTREAM OF THE STEP; EFFECT OF THE SPATIAL RESOLUTION

Downstream of the step, the flow field exhibits a developing a shear layer which starts from the step and subdivides the field into a high velocity and a low velocity region with a reattachment at about  $x/H = 6$  (this value depends on the Reynolds number); the streamlines of such a field are just shown in figure 1, for a Reynolds number equal to about 4100. They also reveal the small counter-rotating region for  $x/H < 1$  which is usually difficult to point out. Even downstream of the step, the measurements are compared with those by other authors and in particular by Tumbiolo *et al.* 1999 obtained using LDA (which satisfactory agreed with those by Kasagi *et al.* (1992) using 3D PTV).

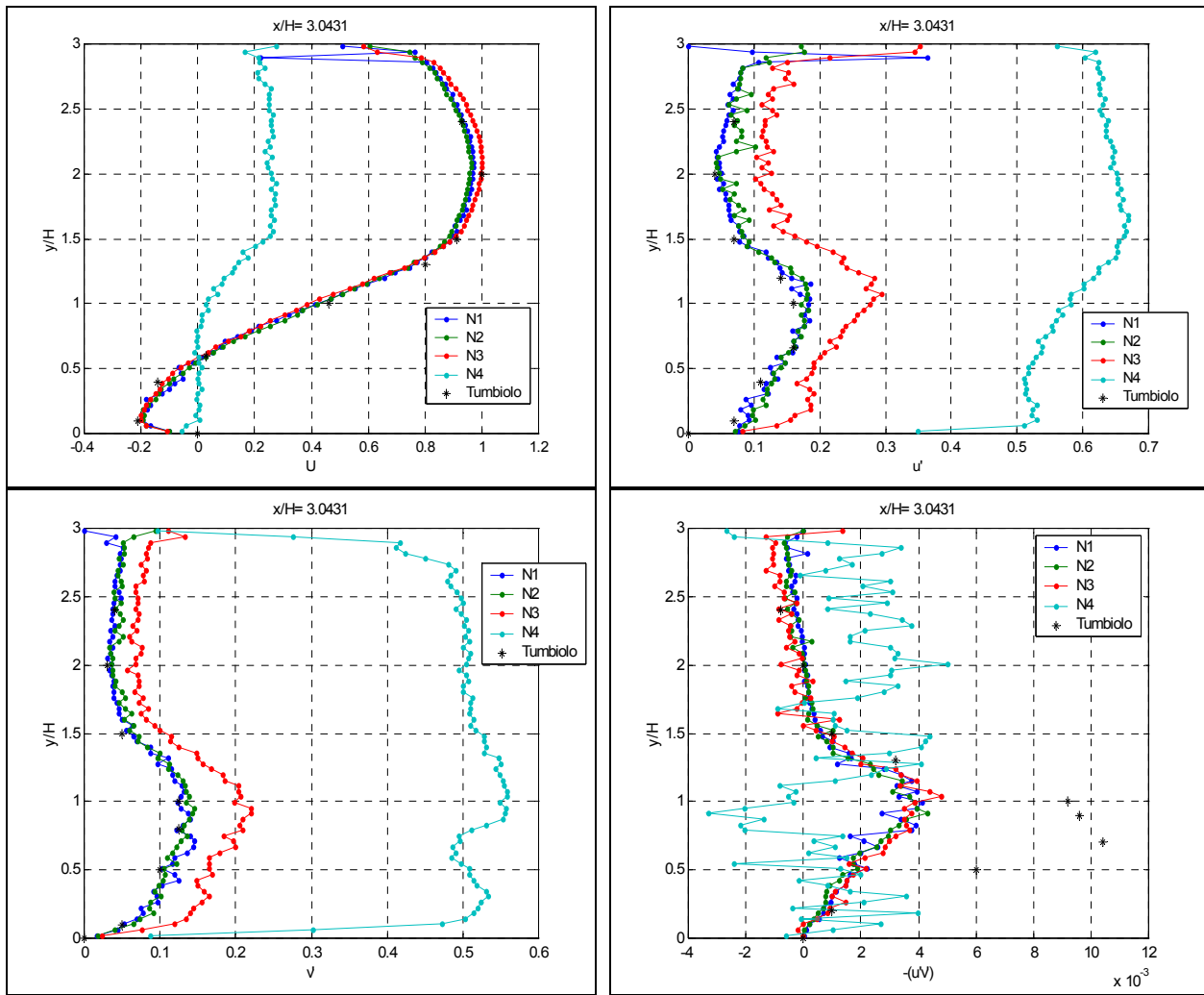


Fig.7. Mean axial velocity, rms axial fluctuation profiles (at the top) and rms vertical fluctuation and Reynolds stress profiles (at the bottom) obtained at four different particle concentrations (equation (1));  $N_1 = 0.56$ ,  $N_2 = 2.59$  and  $N_3 = 7.84$ ,  $N_4 = 18.9$ . Data acquired at  $Re = 4100$  downstream of the step ( $x/D = 3$ ), with the following parameters;  $SR$  (spatial resolution) =  $25 \text{ cm}^{-1}$ ,  $d_{max}/tol$  (ratio between maximum displacement and tolerance) = 5.2,  $thres$  (threshold level) = 40,  $A_{min}$  (minimum particle area) =  $2 \text{ pixel}^2$ . The number of cells used is about 80.



As for the data upstream of the step, the effect of variations in particle concentrations and image analysis parameters are considered; an example of the obtained results is given in figure 7 for a distance from the step  $x/H=3$  with different particle concentrations;  $N_1 = 0.56$ ,  $N_2 = 2.59$ ,  $N_3 = 7.84$  and  $N_4 = 18.9$ . It is important to notice that, in comparison to the measurements upstream of the step, in this case the particle concentrations are much lower. In the profile of the mean axial velocity, the measured velocity deviates from the reference LDA results only for the highest particle concentration ( $N_4$ ); upstream of the step, for a similar value of the concentration, the measured data were still in agreement with the reference numerical data. The measured *rms* profiles reveal that also for the particle concentration characterised by  $N_3$  there is a significant departure from the LDA data. On the Reynolds stress profile, there is also an underestimation of the measured values in comparison to the reference data whatever the particle concentration; this aspect will be considered in connection to the effect of the spatial resolution. The previous results should be regarded by considering that downstream of the step the particle trajectories are not straight (especially in the shear layer and in the reattachment region); therefore, the measured data are much more dependent on the selection of the parameter. Therefore, there is a clear indication for keeping the particle concentration number not larger than the unity, especially in re-circulating regions. As for the particle concentration, also the ratio  $d_{max}/tol$  was changed in a rather restricted interval in comparison to the upstream flow; for values of such a ratio ranging between 2.5 and 9 the obtained results (not shown) agree with those obtained by LDA. These values correspond to maximum turbulence intensities between 10 % and 40 %; the value  $d_{max}/tol = 5$  (corresponding to a maximum turbulent intensity equal to 20 %) is the one which gives the best results in comparison to the LDA data.

The effect of the spatial resolution (*SR*) of the acquiring device is pointed out by enlarging the imaged region of the flow field; in a first series of images the tested flow field extends from  $x/D = 0$  to  $x/D = 3$  (and the spatial resolution was  $SR1 = 25 \text{ cm}^{-1}$ ) whereas in a second test it ranges from  $x/D = 0$  to  $x/D = 5$  (spatial resolution  $SR2 = 15 \text{ cm}^{-1}$ ). In figures 8 and 9 measured profiles of the mean axial velocity, *rms* axial and vertical fluctuations and Reynolds stress are given at different distances from the step with the two previous spatial resolutions. As for the previous parameters, the mean velocity field is almost unaffected by changes in the spatial resolution, while the higher order statistics is much more dependent on such variations. The results on the mean velocity profile agree with those obtained by LDA without any noticeable effect of the spatial resolution; in contrast, the *rms* profiles, show relevant differences which attenuate when moving downstream of the step where the shear layer attains a larger thickness. The data acquired with the highest spatial resolution are always in reasonable agreement with the reference LDA data. This is not true for the Reynolds stress profile which should exhibit a sharp peak at the shear layer locations ( $y/H \approx 1$ ); although the measured Reynolds stress data using the highest spatial resolution strongly improve those obtained at the lowest resolution, they still underestimate the data obtained with LDA (for these data the spatial resolution is in the order of  $100 \text{ cm}^{-1}$ ).

## 5. COMMENTS AND CONCLUSIONS

Measurements of the velocity field upstream and downstream of a backward facing step in fully turbulent conditions are performed by means of Particle Tracking Velocimetry; this flow was chosen as a test case due to the large amount of experimental and numerical data available especially at low Reynolds numbers. The paper is focused on to the determination of the effects which affect the quality of the results both in low and high turbulence intensity regions.

The mean velocity field has been observed to be quite independent on the choice of the acquisition and analysis parameters both upstream and downstream the step, *i.e.* with low and high turbulent intensity, respectively. On the other hand, the second order moments of the velocity fluctuations exhibit much more sensitivity to the choice of those parameters. In low turbulence condition, provided the seeding concentration is low enough, the main effect of changing the analysis parameters is an increase of the noise, that induces a small underestimation of the mean velocity and an overestimation of the variances. Anyway it is worth noting that also a negligible relative error in the mean velocity estimation has meaningful effects on the evaluation of the fluctuations and thus on the computation of the statistical moments. Moreover, from the observation of the results downstream the step is derived that the parameters which are crucial to obtain reliable measurements are those related to the experimental set-up, *i.e.* the seeding concentration and image resolution. In particular the former should be kept low enough ( $N_0$  of order unity) to allow an increase of the tolerance on the successive displacement fluctuations able to capture the turbulent intensity of the flow.

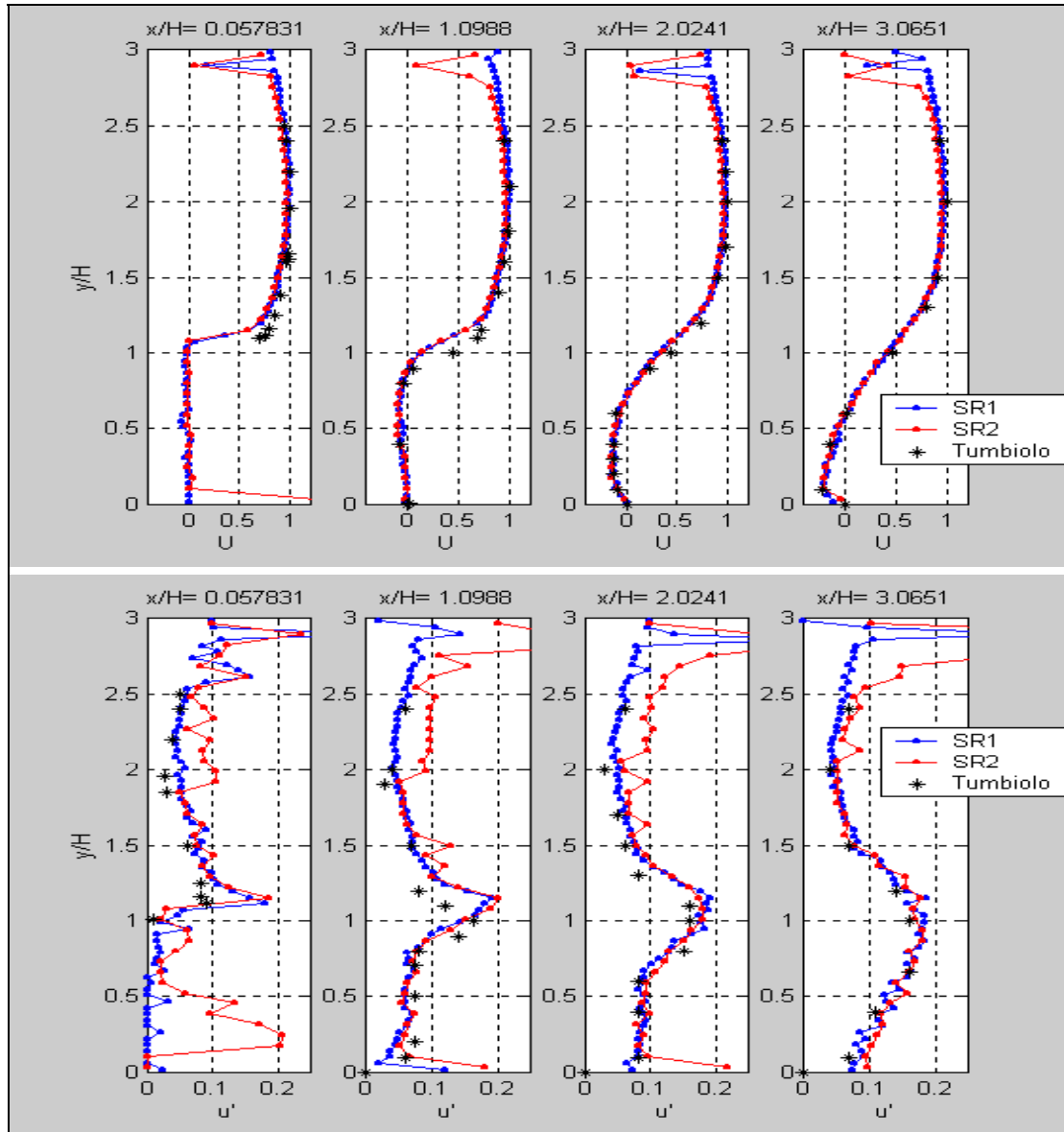


Fig.8. Mean axial velocity (at the top) and rms axial fluctuation profiles (at the bottom) obtained at different distances downstream of the step with two different spatial resolutions;  $SR1 = 25 \text{ cm}^{-1}$ ,  $SR2 = 15 \text{ cm}^{-1}$ . Data acquired at  $Re = 4100$ , with the following parameters;  $d_{\max}/tol = 5$ ,  $N_0$  (particle concentration) = 0.5,  $thres$  (threshold level) = 40,  $A_{\min}$  (minimum particle area) = 2  $\text{pixel}^2$ . The number of cells used is about 80.

## REFERENCES

- Adrian R.J. (1991). "Particle image velocimetry for experimental fluid mechanics", *Annual Review of Fluid Mechanics*, 23, pp. 261-304.
- Armaly B.F., Durst F., Pereira J.C.F. and Schönung B. (1983). "Experimental and theoretical investigation of backward-facing step flow", *Journal of Fluid Mechanics*, 127, pp. 473-496.
- Cenedese A. and Querzoli G. (1997). "Lagrangian statistics and transient matrix measurements by PTV in a convective boundary layer", *Measurement Science and Technology*, 8, pp. 1553-1561.

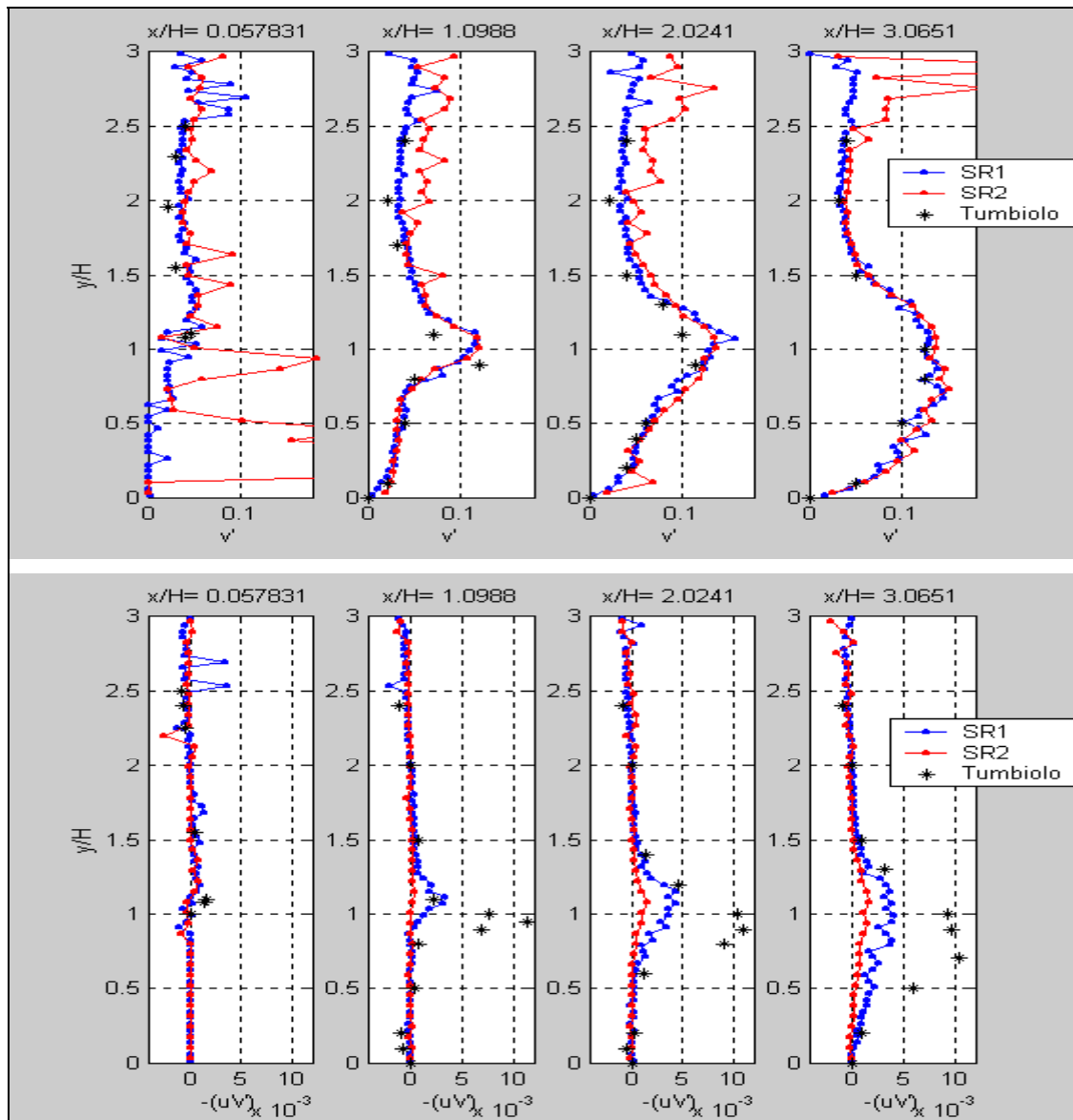


Fig.9. Rms vertical fluctuations (at the top) and Reynolds stress profiles (at the bottom) obtained at different distances downstream of the step with two different spatial resolutions; SR1 = 25 cm<sup>-1</sup>, SR2 = 15 cm<sup>-1</sup>. Data acquired at Re = 4100, with the following parameters;  $d_{max}/tol = 5$ ,  $N_0$  (particle concentration) = 0.5,  $thres$  (threshold level) = 40,  $A_{min}$  (minimum particle area) = 2 pixel<sup>2</sup>. The number of cells used is about 80.

Cenedese A. and Querzoli G. (2000). "Particle tracking velocimetry: measuring in the Lagrangian reference frame", in *Particle image velocimetry and associated techniques*, Von Karman Lecture Series 2000-2001, pp.2.

Di Florio D., Di Felice F. and Romano G.P. (2002). "Windowing, re-shaping and re-orientation of interrogation windows in PIV for the investigation of shear flows", accepted in *Measurement Science and Technology*.

Etheridge D.W. and Kemp P.H. (1978). "Measurement of turbulent flow downstream of a rearward-facing step", *Journal of Fluid. Mechanics*, 66, pp. 545-566.

Huang H.T. and Fiedler H.E. (1997). "A DPIV study of a starting flow downstream of a backward-facing step", *Experiments in Fluids*, 23, pp. 395-404.

- Ishikawa M., Murai Y. and Yamamoto F. (2000). "Numerical validation of velocity gradient tensor particle tracking velocimetry for highly deformed flow fields", *Measurement Science and Technology*, 11, pp. 677-684.
- Kasagi N. and Matsunaga A. (1992). "Turbulence measurement in a separated and reattaching flow over a backward facing step with the aid of a three dimensional particle tracking velocimetry", *Journal of Wind Engineering*, 62, pp.2-7 ([http://ftp.mh.sd.keio.ac.jp/pub/Forced/Comp/fc\\_bs007.csv](http://ftp.mh.sd.keio.ac.jp/pub/Forced/Comp/fc_bs007.csv)).
- Keane R.D., Adrian R.J. and Zhang Y. (1995). "Super-resolution particle image velocimetry", *Measurement Science and Technology*, 6, pp. 754-768.
- Kim J., Moin M. P. and Moser R. (1987). "Turbulence in channel flow at low Reynolds number", *Journal of Fluid Mechanics*, 177, pp. 133-166.
- Le H., Moin P. and Kim J. (1997) "Direct numerical simulation of turbulent flow over a backward-facing step", *Journal of Fluid Mechanics*, 330, pp. 349-374.
- Malik N.A., Dracos T. and Papantoniou D.A.. (1993). "Particle tracking velocimetry in three-dimensional flows – Part 2: Particle tracking", *Experiments in Fluids*, 15, pp. 279-294.
- Nogueira J., Lecuona A. and Rodriguez G. (1999). "Local field correction PIV: on the increase of accuracy of digital PIV systems", *Experiments in Fluids*, 27, pp. 107-116.
- Ohmi K. and Li H.Y. (2000). "Particle-tracking velocimetry with new algorithms", *Measurement Science and Technology*, 11, pp. 607-608.
- Scarano F. and Riethmuller M.L. (1999). "Iterative multigrid approach in PIV image processing with discrete window offset", *Experiments in Fluids*, 26, pp. 513-523.
- Scarano F. and Riethmuller M.L. (2000). "Advances in iterative multigrid PIV image processing", *Experiments in Fluids*, 29, pp. S051-S060.
- Tumbiolo A. (1999). "Experimental study of the flow field downstream a backward facing step", *PhD Thesis in Hydraulics*, University "La Sapienza", Roma.
- Veber P., Dahl J. and Hermansson R. (1997). "Study of the phenomena affecting the accuracy of a video-based Particle Tracking Velocimetry technique", *Experiments in Fluids*, 22, pp. 482-488.
- Westerweel J. (1997). "Fundamentals of digital particle image velocimetry", *Measurement Science and Technology*, 8, pp. 1379-1392.
- Westerweel J. (1999). "Theoretical analysis of the measurement precision and reliability in PIV", *Proceedings of the Third International Conference on PIV*, Santa Barbara, pp. 9-14.